Journal of Materials Chemistry A

Accepted Manuscript

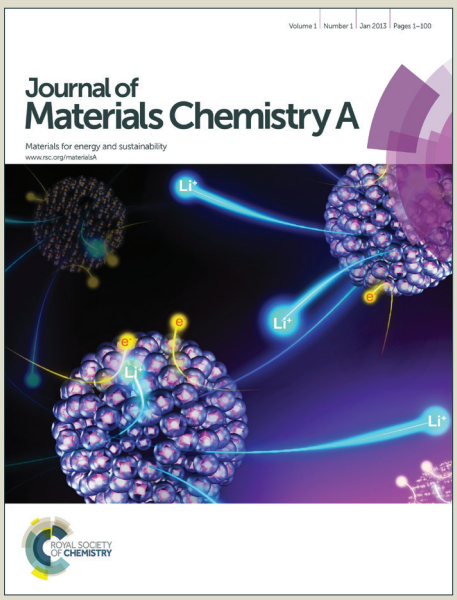

ROYAL SOCIETY OF CHEMISTRY

www.rsc.org/materialsA

Anion exchange membranes composed of perfluoroalkylene chains and ammonium-functionalized oligophenylenes

Hideaki Ono,[ad] Junpei Miyake,[cd] Shigehumi Shimada,[a]
Makoto Uchida,[bd] and Kenji Miyatake*[bcd]

*Corresponding author.
Tel: +81 55 220 8707, E-mail address: miyatake@yamanashi.ac.jp (KM).

Abstract

A novel series of ammonium-containing copolymers (QPAFs) were synthesized as anion exchange membranes for alkaline fuel cell applications. The precursor copolymers (M_w = 28.3 kDa - 90.1 kDa) composed of perfluoroalkylene and phenylene groups were obtained by nickel promoted polycondensation reaction. Chloromethylation and quaternization reactions of the precursors provided thin and ductile QPAF membranes with ion exchange capacity (IEC) ranging from 0.79 to 1.74 meq/g. The QPAF membranes exhibited phase-separated morphology based on the hydrophilic/hydrophobic differences in the main chain structure. The QPAF membrane with optimized copolymer composition and IEC = 1.26 meq/g showed high hydroxide ion conductivity (95.5 mS/cm in water at 80 °C), excellent mechanical properties (large elongation at break (218%)), and reasonable alkaline stability in 80 °C. Alkaline fuel cell using the QPAF used as the membrane and electrode binder achieved the maximum power density of 139 mW/cm^2 at a current density of 420 mA/cm^2.

1. Introduction

Fuel cells have attracted considerable attention as a promising energy conversion device for addressing global environmental issues. Among the several kinds of fuel cells, polymer electrolyte fuel cells (PEFCs) using proton conductive polymer membranes are attractive for the applications in electric vehicles and residential co-generation system. Currently, perfluorinated sulfonic acid polymers such as Nafion (Du Pont) are most used due to their high proton conductivity and chemical and mechanical stability. However, because of the strongly acidic nature of the membrane, PEFCs require expensive platinum as electrocatalyst which is a serious drawback for the wide-spread practical applications.[1-3]

A potential breakthrough is the use of anion exchange membranes (AEMs) to replace PEMs. The basic conditions of anion exchange membrane fuel cells (AEMFCs) enable the use of abundant non-precious metals such as Ni, Co, and Fe as the electrocatalyst. Moreover, kinetics of the oxygen reduction reaction is better in alkaline than in acid. In the last decade, there have been considerable efforts in developing better performing anion exchange membranes.[4-8] Ammonium-functionalized aromatic polymers have been most studied, and some are claimed to exhibit high hydroxide ion conductivity.[9-11] We found that multiblock copolymer poly(arylene ether sulfone ketone)s exhibited high hydroxide ion conductivity (144 mS cm^{-1} at 80 °C in water) due to high density of ammonium groups in the hydrophilic block and well-developed ionic channels. However, the alkaline stability of the ammonium-functionalized aromatic polymers remains an issue.[12,13] Kim et al. and Ramani et al. reported that the main chain degradation of quaternized poly(arylene ether)s was triggered by the attack of hydroxide ions at the phenylene carbons *ipso* to the ether bonds.[14-16] More recently, in order to improve the alkaline stability, we have developed aromatic copolymer membranes (QPE-bl-9) containing ammonium-functionalized

oligophenylene moieties as the hydrophilic component. The membrane exhibited high hydroxide ion conductivity (138 mS cm^{-1} at 80 °C in water) and reasonable alkaline stability at 1 M KOH aqueous solution for 1000 h at 40 °C.[17]

In this paper, we report advanced version of our aromatic copolymer membranes (QPAF) composed of perfluoroalkylene chains as the hydrophobic component and the quaternized oligophenylene groups as the hydrophilic component and thus, no heteroatom linkages (such as ether, sulfone, and ketone groups) were included in the polymer main chains. The introduction of the highly hydrophobic perfluoroalkylene chains are expected to provide AEMs with improved ion conductivity, mechanical properties, and solvent solubility. Their synthesis, structure, properties (hydroxide ion conductivities, water uptake, gas permeability, and mechanical properties), alkaline stability, and hydrogen/oxygen fuel cell performance have been investigated in detail. Since QPAF membranes contained the perfluoroalkylene groups in the main chain, their properties are compared to those of the perfluorinated sulfonic acid polymer, Nafion, membrane.

2. Experimental details

2.1 Materials.

Perfluoro-1,6-diiodohexane (> 98%, TCI), perfluoro-1,4-diiodobutane (> 95%, TCI) 1-chloro-3-iodobenzene (> 97%, TCI), copper (Cu) powder (particle size 75-150 μm, > 99%, Kanto Chemical), dimethyl sulfoxide (DMSO) (> 99%, Kanto Chemical), 1,3-dichlorobenzene (> 98%, TCI), 1,4-dichlorobenzene (> 99%, TCI), 2,2'-bipyridine (> 99%, TCI), bis(1,5-cyclooctadiene)nickel(0) ($Ni(COD)_2$) (> 95%, Kanto Chemical), N,N-dimethylacetamide (DMAc) (> 99%, Kanto Chemical), chloromethyl methyl ether (CMME) (> 95%, TCI), zinc

chloride ($ZnCl_2$) (> 98% Kanto Chemical), thionyl chloride ($SOCl_2$) (> 98%, TCI), 1,1,2,2-tetrachloroethane (TCE) (> 98%, Kanto Chemical), 45wt% trimethylamine aqueous solution (Aldrich) were used as received. Other chemicals were of commercially available grade and used as received.

2.2 Synthesis of Perfluoroalkylene Monomers.

A 100 mL three-necked flask equipped with a nitrogen inlet was charged with perfluoro-1,6-diiodohexane (5.54 g, 10.0 mmol), 1-chloro-3-iodobenzene (11.9 g, 50.0 mmol), Cu powder (9.53 g, 150 mmol) and DMSO (60 mL). The mixture was heated at 120 °C for 48 h. After the reaction, the mixture was poured into 300 mL of 0.1 M nitric acid to precipitate a gray powder. The crude product was collected by filtration and dissolved in 300 mL of methanol. The solution was filtered with a PTFE membrane filter (0.45 μm pore size, omnipore). The gray solid was washed several times with methanol. Into the combined filtrate, 500 mL of deionized water was poured slowly to precipitate a white crystalline powder. The product was washed with 1/1 (by volume) mixture of methanol and water several times and dried at 60 °C in a vacuum oven to obtain pure perfluoroalkylene monomer **1** (x = 6) in 85% yield. The shorter chain length perfluoroalkylene monomer **1** (x = 4) was prepared in a similar manner from perfluoro-1,4-diiodobutane (30% yield).

2.3 Polymerization.

A typical procedure is as follows. A 100 mL three-necked flask equipped with a nitrogen inlet and a mechanical stirrer was charged with the monomer **1** (x = 6) (5.42 g, 10.4 mmol), 1,3-dichlorobenzene (0.73 g, 4.99 mmol), 1,4-dichlorobenzene (0.95 g, 6.44 mmol), 2,2'-bipyridine (8.52 g, 54.5 mmol) and DMAc (55 mL). The mixture was heated at 80 °C to obtain a homogeneous solution. To this mixture, $Ni(COD)_2$ (15.0 g, 54.5 mmol) was added. After the

polymerization for 3 h, the mixture was poured into 300 mL of methanol to precipitate a black powder. The crude product was treated with concentrated hydrochloric acid overnight, washed with water and methanol several times, and dried at 60 °C in a vacuum oven to obtain a white powdery product (PAF(C6)-2 (*m*1.00*n*0.48*o*0.62)) in 82% yield.

2.4 Chloromethylation of PAF(C6)-2.

A typical procedure is as follows. A 100 mL round-bottomed flask equipped with a condenser was charged with PAF(C6)-2 (*m*1.00*n*0.48*o*0.62) (4.20 g) and TCE (43 mL). After dissolution of the polymer, CMME (87 mL, 125 equimolar to phenylene unit in the hydrophilic moieties of the polymer), $SOCl_2$ (13 mL, 20 equimolar to phenylene unit in the hydrophilic moieties of the polymer), and $ZnCl_2$ (1.18 g, equimolar to phenylene unit in the hydrophilic moieties of the polymer) were added into the mixture. The mixture was heated at 80 °C for 24 h and poured into 800 mL of methanol to precipitate a white powder. The crude product was washed with methanol several times and dried at 60 °C in a vacuum oven to obtain a chloromethylated polymer (CMPAF(C6)-2 (*m*1.00*n*0.48*o*0.62)) in 97% yield.

2.5 Quaternization of CMPAF(C6)-2.

CMPAF(C6)-2 (*m*1.00*n*0.48*o*0.62) (2.00 g) was dissolved in 60 mL of 45 wt% trimethylamine aqueous solution. The mixture was stirred for 48 h at room temperature. Then, the mixture was poured into 240 mL of 2 M HCl to neutralize the excess trimethylamine. The mixture was dialyzed and evaporated to dryness to obtain a brown solid (QPAF(C6)-2 (*m*1.00*n*0.48*o*0.62)) in 98% yield.

2.6 Membrane Preparation.

QPAF(C6)-2 (2.00 g) was dissolved in 30 mL of DMSO. The solution was filtered with a syringe stuffed with cotton and cast onto a flat glass plate. Drying the solution at 80 °C overnight gave a transparent light brown membrane (ca. 50 μm thick).

2.7 Measurements.

^{1}H-NMR spectra were obtained on a JEOL JNM-ECA/ECX500 using deuterated chloroform ($CDCl_3$) or deuterated dimethyl sulfoxide (DMSO-d_6) as a solvent and 0.03% tetramethylsilane (TMS) as an internal reference. Molecular weight was measured with gel permeation chromatography (GPC) equipped with two Shodex K-805 L columns and a Jasco 805 UV detector (270 nm) with DMF containing 0.01 M LiBr as eluent. Molecular weight was calibrated with standard polystyrene samples. For transmission electron microscope (TEM) observation, a piece of the membrane was stained with tetrachloroplatinate ions by ion exchange of the ammonium groups in 0.5 M K_2PtCl_4 aqueous solution at 60 °C, and dried in a vacuum oven overnight at 60 °C. The stained membrane sample was embedded in epoxy resin, sectioned to 50 nm thickness with a Leica microtome Ultracut UCT, and placed on copper grids. Images were taken on a Hitachi H-9500 transmission electron microscope with an accelerating voltage of 200 kV.

Ion exchange capacity (IEC) was determined by titration. The membrane samples (ca. 50 mg) in chloride ion forms were immersed in 12.5 mL of 0.1 M $NaNO_3$ for 24 h. The amount of Cl^- released from the membranes was measured by titration with 0.01 M $AgNO_3$ using K_2CrO_4 as an indicator and $NaHCO_3$ as a pH adjuster. The hydroxide ion conductivities of the membranes were measured in degassed, deionized water (18 MΩ) at 30, 40, 60, and 80 °C using a 4-probe conductivity cell attached with an AC impedance spectroscopy (Solartron 1255B, Solartron Inc.). Ion conducting resistances (R (Ω)) were determined from the impedance plots obtained in the

frequency range from 1 to 10^5 Hz. The hydroxide ion conductivity (σ) was calculated from the equation, $\sigma = l/AR$, where A (cm^2) and l (cm) are the cross-section area of the membrane and the distance between two reference electrodes, respectively. Water uptake was measured in deionized water at room temperature for 24 h. Drying the membranes in a vacuum oven at 80 °C provided a dry weight (W_d). Wet weight (W_w) was measured after the surface water was carefully wiped off with paper. The water uptake was calculated using the following equation: Water uptake (%) = $(W_w - W_d) / W_d \times 100$. The ion conductivity and water uptake of the membranes in chloride ion form were measured under N_2 with controlled humidity with a Bel Japan solid electrolyte analyzer system MSB-AD-V-FC equipped with a chamber, a magnetic suspension balance, and a 4-probe conductivity cell. The chloride ion conductivities were measured after equilibrating for at least 1 h at set temperature and humidity by using an AC impedance spectroscopy (Solartron 1255B, Solartron Inc.). For water uptake measurement, membrane samples were set in a chamber and dried at 80 °C under vacuum for 3 h to obtain dry weight, and the wet weight was collected after equilibrating for at least 1 h at set temperature and humidity.

Alkaline stability test of the membranes was performed in 1 M KOH aqueous solution at 60 and 80 °C. The hydroxide ion conductivity was recorded in degassed water at 40 °C as a function of testing time. The post-test membranes were analyzed by IR spectra.

Gas permeability was measured using a GTR-Tech 20XFYC gas permeation measurement apparatus containing a Yanaco G2700T gas chromatography with a Porapak-Q column and a TCD detector. Argon and helium were used as a carrier gas for the measurement of hydrogen and oxygen, respectively. A membrane sample in chloride ion form (40 mm in diameter and 50 μm thick) was set in a cell that had a gas inlet and an outlet on both sides of the membrane. On one side of the membrane, hydrogen or oxygen test gas was supplied at a flow rate of 30 mL/min,

while on the other side of the membrane, the same gas as the carrier used in the gas chromatograph (flow gas) was supplied at a flow rate of 20 mL/min and both side of gases were dried or humidified under the same conditions to ensure homogeneous wetting of the membrane sample. Then, 7.4 mL of flow gas was sampled and subjected to the gas chromatography to quantify the test gas permeated through the membrane. The measurement was repeated until stable permeation data were obtained at least for 5 h. Gas permeation coefficient, Q (cm^3 (STD) cm/cm^2 s cmHg) was calculated by following equations: $Q = 273/T \times 1/A \times B \times 1/t \times 1/(76\text{-}P_{H2O})$, where T (K) is the absolute temperature of the cell, A (cm^2) is the permeation area, B (cm^3) is the amount of permeated test gas, t (s) is the sampling time, l (cm) is the thickness of the membrane and P_{H2O} (cmHg) is the water vapor pressure.

Dynamic mechanical analysis (DMA) was carried out with an ITK DVA-225 dynamic viscoelastic analyzer. Temperature dependence of storage modulus (E'(Pa)), loss modulus (E"(Pa)), and tan δ at 60% RH and 10 Hz was obtained for the membranes (5 × 30 mm) between r.t. and 95 °C at a heating rate of 1 °C/min.

Tensile strength testing was carried out with a Shimadzu universal testing instrument Autograph AGS-J500N equipped with a temperature and humidity controllable chamber. The samples were cut into a dumbbell shape (35 × 6 mm (total) and 12 × 2 mm (test area)). Stress strain curves were obtained at 80 °C and 60% RH at a stretching rate of 10 mm/min after equilibrating the membrane at least for 3 h.

2. 8 Preparation of Catalyst Coated Membrane (CCM) and Fuel Cell Operation.

Pt (50 wt%) catalysts supported on carbon black (0.80 g) (TEC10E50E, Tanaka Kikinzoku Kogyo), water (3.30 g), and ethanol (3.30 g) were mixed by a planetary ball mill at 270 rpm for 30 min. After adding 5 wt% QPAF(C6)-2 solution in ethanol (6.80 g), the mixture was further

mixed by a ball mill for 30 min at 270 rpm and by a pot mill for 12 h. The mass ratio of the dried ionomer and carbon black was adjusted to be 0.8. The slurry thus obtained was sprayed onto both sides of the QPAF(C6)-2 or QPAF(C6)-4 membrane (54 μm thick) and pressed at 10 kgf/cm^2 at r.t. for 3 min to obtain a catalyst coated membrane (CCM). The coated area was 4.4 cm^2. The Pt loading in the catalyst layer was ca. 0.20 mg/cm^2 for each electrode. The CCM was treated with 1.0 M KOH for 48 h for ion exchange and with deionized water for 24 h to remove residual KOH. The treated CCM was mounted in a single cell with a gas diffusion layer and a gasket. Prior to the measurement, fully humidified hydrogen and nitrogen was supplied to the anode and cathode, respectively. The fuel cell was operated at 40 °C or 60 °C with supplying full humidified H_2 and O_2 gas at a flow rate of 100 mL/min to the anode and the cathode, respectively. The high-frequency resistance (HFR) of the cell was measured with a Kikusui FC impedance meter 2150 at 5.0 kHz.

3. Results and Discussion

3.1 Synthesis of Copolymers and Membranes.

The title quaternized copolymers were synthesized as shown in **Scheme1**. Hydrophobic monomers **1** (x = 4, 6) were synthesized by the Ullmann coupling reaction of 1,4-diiodo-octafluorobutane or 1,6-diiodo-dodecafluorohexane and 1-chloro-3-iodobenzene using Cu powder as the catalyst.[18,19] 3 - 5 Times excess of 1-chloro-3-iodobenzene was used to prevent oligomerization of the diiodides and to ensure the formation of chlorine-terminated monomers. The mixture solvent of methanol and water (1/1 by volume) was effective in dissolving the excess 1-chloro-3-iodobenzene and isolating the monomers. The monomer **1** (x = 6) was obtained in high yield (85%) and purity (> 99% by ^{1}H NMR). The monomer **1** (x = 4) was obtained in

lower yield (30 %) because of more solubility in the mixture solvent of methanol and water. The monomers **1** were characterized by ^{1}H and ^{19}F NMR spectra, in which all peaks were well-assigned to the supposed chemical structure (**Fig. S1** in the ESI †).

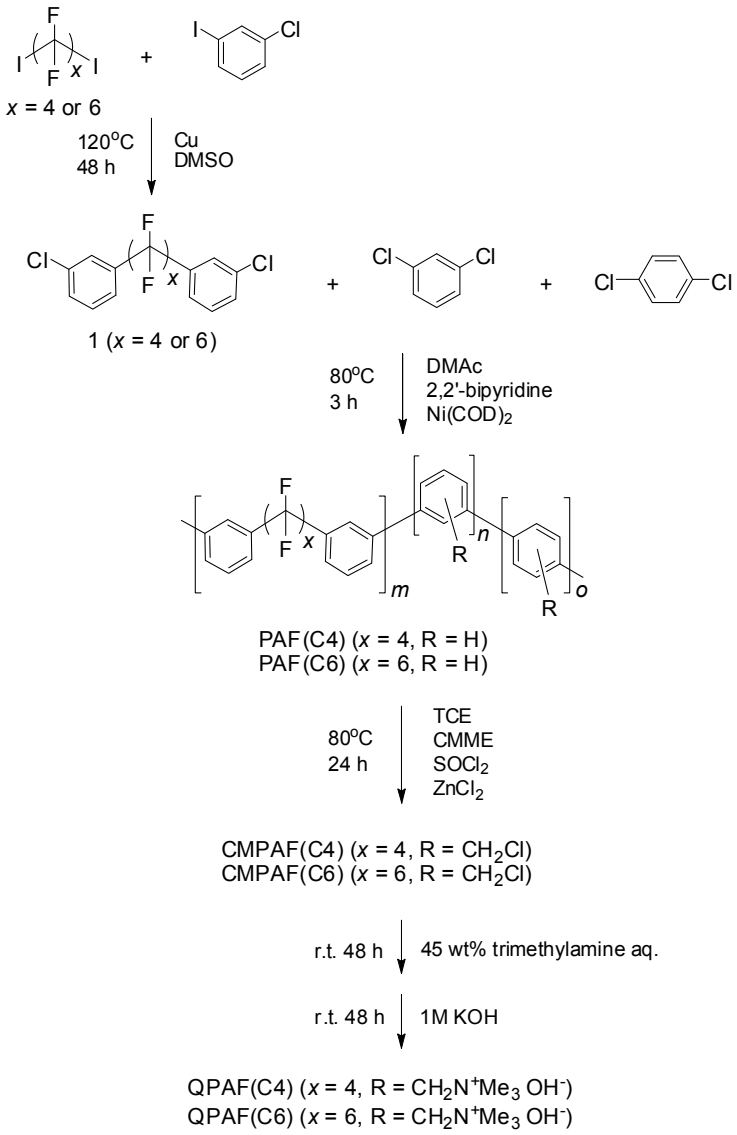

Scheme 1. Synthesis of QPAF(C4) and QPAF(C6)

The precursor copolymers PAF(C4, C6) were synthesized by Ni-promoted polycondensation reaction of the monomers **1** and dichlorobenzene. Our initial investigation with *p*-

dichlorobenzene (without *m*-dichlorobenzene) failed and provided insoluble low molecular weight product. Therefore, we have determined to use the mixture of *p*-dichlorobenzene and *m*-dichlorobenzene. In order to evaluate the effect of copolymer composition on the properties of the quaternized copolymers, a series of copolymers PAF(C6)-1 ~ 7 were synthesized with changing the feed molar ratio of *m* (monomer **1**, x = 6), *n* (*m*-dichlorobenzene), and *o* (*p*-dichlorobenzene). The reaction proceeded successfully to provide high molecular weight copolymers PAF(C6) as a white powder. The obtained copolymers were soluble in some organic solvents such as chloroform, TCE, and DMAc. The molecular weight of the copolymers estimated from GPC analyses were M_n = 5.0 – 14.0 kDa and M_w = 28.3 – 90.1 kDa, respectively (**Table 1**). The molecular weight increased with increasing the content of *m*-phenylene moieties possibly because of better reactivity of *m*-dichlorobenzene than that of *p*-dichlorobenzene. The results are not consistent with our previously reported copolymerization of chlorine-terminated oligomers, *m*- and *p*-dichlorobenzene.[17] The reactivity of dichlorobenzene in Ni-promoted polycondensation might change with the other comonomers. Monomer **1** (x = 4) with shorter perfluoroalkylene groups also provided high molecular weight copolymer (M_n = 8.2 kDa and M_w = 74.8 kDa). The chemical structure of the copolymers was analyzed by ^{1}H NMR spectra. A typical example is shown in **Fig. 1a** for PAF(C6)-2 (*m*1.00*n*0.48*o*0.62). Close examination of the ^{1}H NMR spectra of the copolymers with different compositions enabled us to assign the aromatic protons (see **Fig. S2** for details in the ESI †). The copolymer compositions estimated from the ^{1}H NMR spectra were in good accordance with those of the feed comonomer ratios (**Table 1**). In most cases, *m*-phenylene content was slightly higher than *p*-phenylene content, supporting the above mentioned idea on higher reactivity of meta isomer. In the ^{19}F NMR spectra of the copolymers, all peaks were similar to those of the monomers **1** suggesting no reactions in the

perfluoroalkylene groups during the polycondensation reaction (**Fig. S3a** in the ESI †).

Friedel-Crafts chloromethylation reaction of the copolymers PAF(C4, C6) was carried out with CMME using $ZnCl_2$ as a Lewis acid catalyst and $SOCl_2$ as a promoter.[20] The chloromethylated copolymers CMPAF(C4, C6) were recovered as a white powder similar to the parent copolymers. The obtained CMPAFs showed somewhat better solubility in organic solvents. The GPC profiles of CMPAFs were similar to those of the parent copolymers, suggesting no detectable side-reactions such as cross-linking during the chloromethylation reaction (**Fig. S4** in the ESI †). From the ^{1}H NMR spectra of CMPAF(C6)-2, new peaks appeared at 4.0 – 5.0 ppm assignable to methylene protons of the chloromethyl groups (**Fig. 1b**). The peaks were multiplets indicating that the chloromethyl groups were substituted at several different positions on the 1,3- and 1,4-phenylene groups. The result is similar to our previously reported copolymers sharing the same phenylene components.[17] To evaluate the reactivity of the phenylene rings attached to the perfluoroalkylene groups, a model homopolymer was prepared from the monomer **1** and subjected to the chloromethylation reaction under the same conditions. The recovered product did not exhibit changes in the ^{1}H NMR (**Fig. S5** in the ESI †) and ^{19}F NMR spectra from those of the parent model polymer, suggesting the inertness of the phenylene rings attached to the electron-withdrawing perfluoroalkylene chains. The degree of chloromethylation (DC defined as a number of chloromethyl groups per phenylene unit) values were estimated from the integral ratios of aromatic peaks (8.0 – 7.4 ppm) to methylene peaks (5.0 – 4.0 ppm) in the ^{1}H NMR spectra and are summarized in **Table 1**. The DC values ranged from 0.65 to 0.87 and were unlikely dependent on the copolymer composition.

Quaternization reaction of CMPAF(C4, C6) copolymers were carried out in trimethylamine aqueous solution. Since CMPAFs were soluble in the trimethylamine solution, the quaternization

reaction proceeded in a homogeneous mixture. Once recovered copolymers were no longer soluble in water but in polar organic solvents such as DMSO, methanol, and ethanol. Solubility in alcohol would be derived from the perfluoroalkylene groups. Perfluorinated sulfonic acid polymers such as Nafion are also soluble or form dispersion in alcohols. The chemical structure of QPAF copolymers were analyzed by ^{1}H NMR spectra. As shown in **Fig. 1c** for QPAF(C6)-2, large multiplet peaks were observed at ca. 2.9 ppm assignable to the ammoniomethyl groups. The methylene peaks were broader and appeared at slightly lower magnetic field than those of the parent CMPAF copolymers because of the strong electron-withdrawing nature of the ammonium groups. The integral ratio of the peak 2 to whole aromatic proton peaks was in good accordance with the one calculated from the DC value, indicating quantitative quaternization reaction of the chloromethyl groups. The IEC values were also obtained by titration, which were in good accordance with those estimated from the ^{1}H NMR spectra within acceptable errors (**Table 1**).

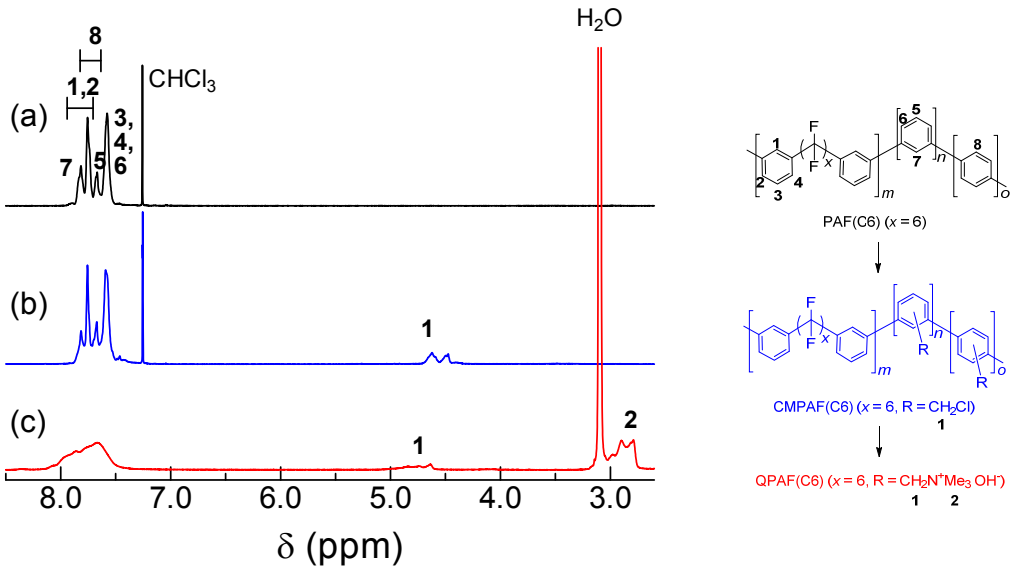

Fig. 1. ^{1}H NMR spectra of (a) precursor copolymer PAF(C6)-2 (x = 6, m1.00n0.48o0.62) in $CDCl_3$, (b) CMPAF(C6)-2 in $CDCl_3$, and (c) QPAF(C6)-2 in DMSO-d_6.

Table 1. Composition, molecular weight, degree of chloromethylation (DC), and ion exchange capacity (IEC) of the QPAF polymers

No.	Composition							Molecular Weight (kDa)[c]		DC[d]	IEC (meq/g)	
	x	*m*[a]	*n*[a]	*o*[a]	*m*[b]	*n*[b]	*o*[b]	M_n	M_w		^{1}H NMR	titration
(C4)-1	4	1.00	0.48	0.62	1.00	0.29	0.38	8.2	74.8	0.76	1.18	1.11
(C6)-1	6	1.00	0.24	0.56	1.00	0.17	0.40	5.0	28.3	0.65	0.78	0.86
(C6)-2	6	1.00	0.48	0.62	1.00	0.41	0.53	9.1	49.0	0.72	1.14	1.26
(C6)-3	6	1.00	0.72	0.68	1.00	0.71	0.67	17.7	66.6	0.76	1.50	1.52
(C6)-4	6	1.00	0.96	0.74	1.00	1.05	0.81	7.0	90.1	0.73	1.79	1.74
(C6)-5	6	1.38	0.48	0.62	1.38	0.36	0.47	14.0	33.7	0.71	0.72	0.79
(C6)-6	6	0.79	0.48	0.62	0.79	0.42	0.55	13.7	59.4	0.87	1.54	1.58
(C6)-7	6	0.65	0.48	0.62	0.65	0.47	0.61	9.1	51.3	0.69	1.52	1.61

[a] Calculated from the feed comonomer ratio. [b] Determined from the ^{1}H NMR spectra of the PAF polymers. [c] As PAF analyzed by GPC (calibrated with polystyrene standard). [d] Degree of chloromethylation = (number of chloromethyl group/hydrophilic repeat unit) calculated from the ^{1}H NMR spectra.

3.2 Morphology of the Quaternized Membrane.

Fig. 2 shows cross-sectional TEM image of the QPAF(C6)-2 membrane (IEC = 1.26 meq/g) stained with tetrachloroplatinate ions. The dark areas represent hydrophilic domains composed of stained ammonium groups and their aggregates. The hydrophilic domains were spherical of ca. 1.6 nm in diameter. Compared to our previous quaternized copolymer QPE-bl-9 (ca. 2.0 nm) membrane (see **Fig. S6** for chemical structure in the ESI †) containing the same hydrophilic components but different hydrophobic block (partially fluorinated arylene ether),[17] the hydrophilic domains of the QPAF membrane were slightly smaller. The hydrophobic domains of QPAF (ca. 1.0 nm) were also smaller than those of the QPE-bl-9 membrane (ca. 1.5 nm). Such

small phase separation would reflect the random copolymer structure of the QPAF. For reference, Nafion membrane which is also a random copolymer is well-known to have spherical hydrophilic domains (ca. 4 - 5 nm) surrounded by hydrophobic domains of similar size. It is considered that the flexible perfluoroalkylene main chains with no aromatic moieties contributed to slightly larger hydrophilic/hydrophobic phase separation in the Nafion membrane.

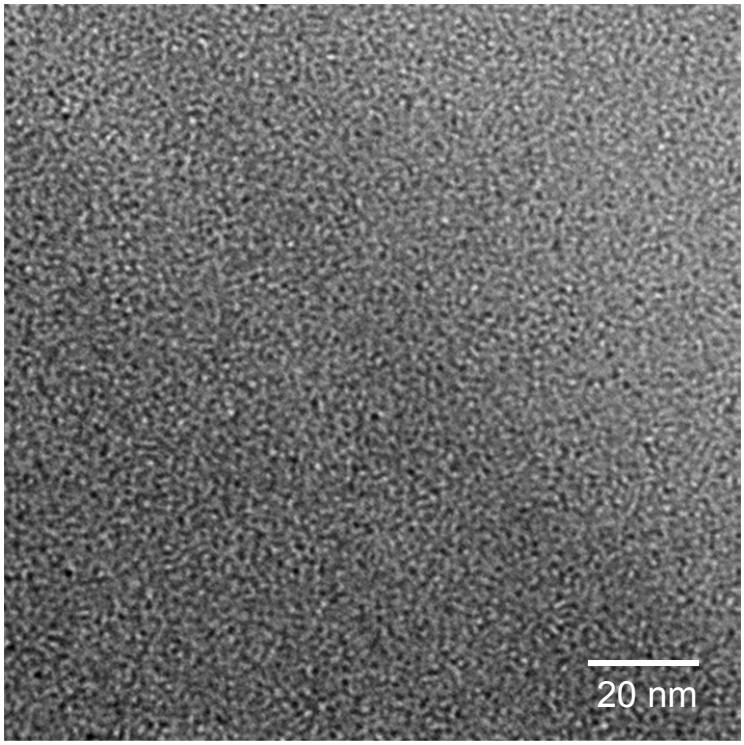

Fig. 2. TEM image of QPAF(C6)-2 membrane (IEC = 1.26 meq/g) stained with tetrachloroplatinate ions.

3.3 Water Uptake and Ion Conductivity.

Fig. 3 shows water uptake and hydroxide ion conductivity of QPAF membranes in water as a function of IEC. For comparison, data for the QPE-bl-9 membrane are also included.[17] Water uptake increased as increasing IEC values for both series of the membranes since water molecules would be mostly absorbed with the hydrophilic ammionium groups. QPAF membranes exhibited larger water uptake than that of the QPE-bl-9 membranes. This was more pronounced for higher IEC membranes. The water uptake was re-plotted as λ (number of water molecules per ammonium group) in **Fig. 4,** which shows that λ jumped for QPAF membranes with IEC values greater than 1.5 meq/g while λ was nearly constant for QPE-bl-9 membranes. The results suggest that the QPAF membranes swell more than QPE-bl-9 membranes probably because of the smaller content of rigid aromatic groups and the flexibility of perfluoroalkylene chain in the hydrophobic component. Similar to the water uptake behavior, QPAF membranes showed somewhat higher hydroxide ion conductivity than that of QPE-bl-9 membranes when IEC was lower than ca. 1.5 meq/g. For example, QPAF(C6)-2 with 1.09 meq/cm^3 of volumetric wet IEC (taking the density,1.41 g/cm^3, and water uptake, 45 wt%, into account) exhibited 49.6 mS/cm and QPE-bl-9 with 1.14 meq/cm^3 of volumetric wet IEC (taking the density,1.30 g/cm^3, and water uptake, 37 wt%, into account) exhibited 22.5 mS/cm. The conductivity dropped at higher IEC for QPAF membranes possibly because high water uptake and swelling caused lower carrier ion concentration. It seemed that QPAF(C6)-2 (designated in star plot) exhibited best balanced properties with high ion conductivity and reasonable water uptake.

Temperature dependence of hydroxide ion conductivities of the selected QPAF(C4, C6) and QPE-bl-9 membranes in water is shown in **Fig. 5**. All membrane samples exhibited Arrhenius-type temperature dependence of the ion conductivity up to 80 ºC. QPAF(C6)-2 membrane (IEC =

1.26 meq/g) achieved the highest hydroxide ion conductivity (95.5 mS/cm at 80 °C), which was ca. 2.2 times higher than that (44.4 mS/cm at 80 °C) of QPE-bl-9 membrane with comparable IEC (1.3 meq/g). Apparent activation energy for the hydroxide ion conduction of QPAF membranes was estimated from the slope to be 9.2 - 12.1 kJ/mol, similar to the reported values for AEMs.[10,13,17] The proton conductivity of the commercial Nafion NRE 212 membrane (IEC = 0.91 meq/g) was measured under the same conditions and is included in **Fig. 5**. Nafion exhibited similar temperature dependence of the ion conductivity to that of QPAF membranes. The apparent activation energy for the proton conduction of Nafion was 10.3 kJ/mol. The proton conductivity of Nafion was ca. 1.9 times higher than that of QPAF(C6)-2 membrane. The volumetric ion exchange capacities taking the density of each membrane into account (d = 1.41 g/cm^3 for QPAF(C6)-2 and 1.98 g/cm^3 for Nafion) were 1.78 meq/cm^3 for QPAF(C6)-2 and 1.80 meq/cm^3 for Nafion, respectively. Assuming single ion conduction, molar ion conductivities were roughly estimated to be 28 S cm^2/mol for OH^- in QPAF(C6)-2 and 55 S cm^2/mol for H^+ in Nafion.

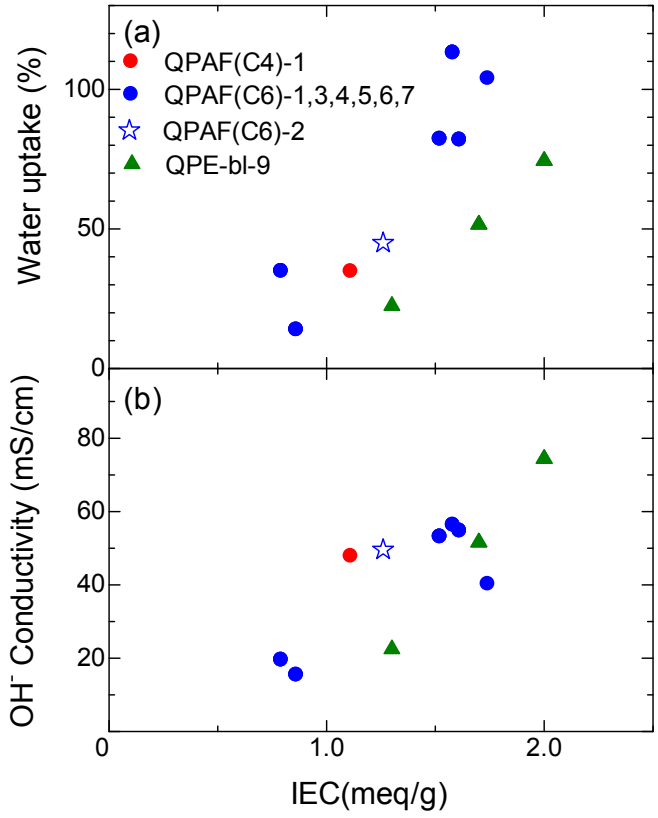

Fig. 3. (a) Water uptake at room temperature and (b) hydroxide ion conductivity at 30 °C of QPAF and QPE-bl-9 membranes as a function of IEC.

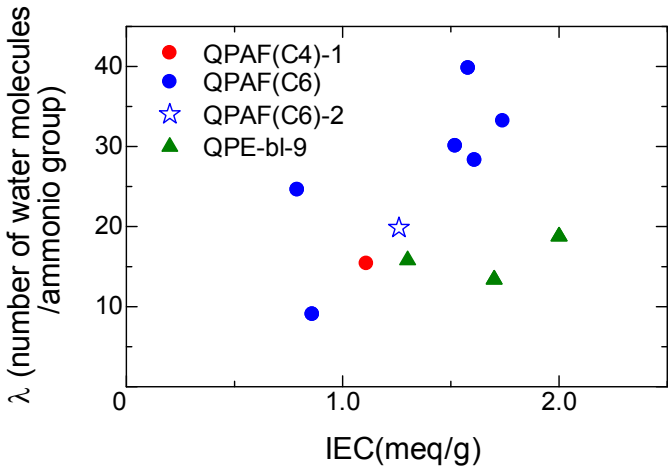

Fig. 4. λ of QPAF(C4, C6) and QPE-bl-9 membranes as a function of IEC.

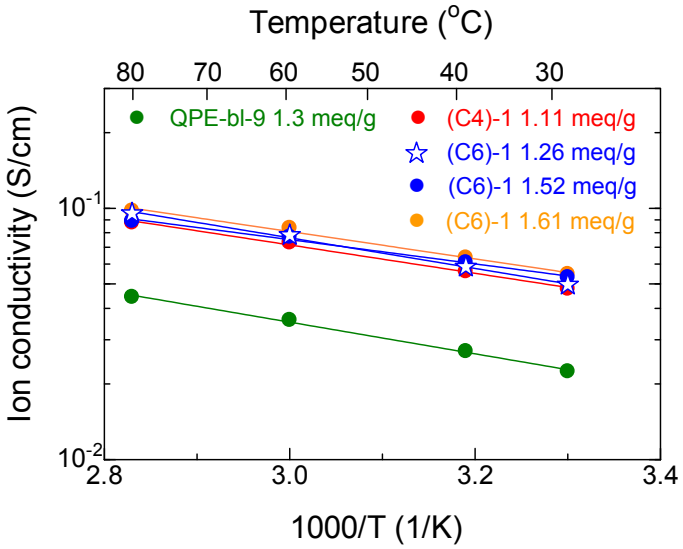

Fig. 5. Temperature dependence of ion conductivity of QPAF(C4, C6) and QPE-bl-9 (both in OH^- form) membranes in water.

Humidity dependence of water uptake and Cl^- conductivity of QPAF(C6)-2 and -4 membranes (IEC = 1.26 and 1.74 meq/g, respectively) was measured at 80 °C and is summarized in **Fig. 6**. Water uptake of the two QPAF membranes increased with increasing relative humidity and reached 16.4 % and 21.0 % at 95% RH for (C6)-2 and (C6)-4, respectively. Compared to those in liquid water at room temperature (**Fig. 3**), the water uptake of the QPAF membranes and the differences in the water uptake between two membranes were much smaller under the humidified nitrogen at 80 °C. The low swellability of QPAF membranes under humidified conditions would be beneficial for practical fuel cell applications. Similar to hydroxide ion conductivity in water, the chloride ion conductivity of the two QPAF membranes was comparable at high RH. Large increase in water uptake for QPAF membrane with IEC higher than 1.5 meq/g would cause lower ion concentration to account for less effective ion conduction.

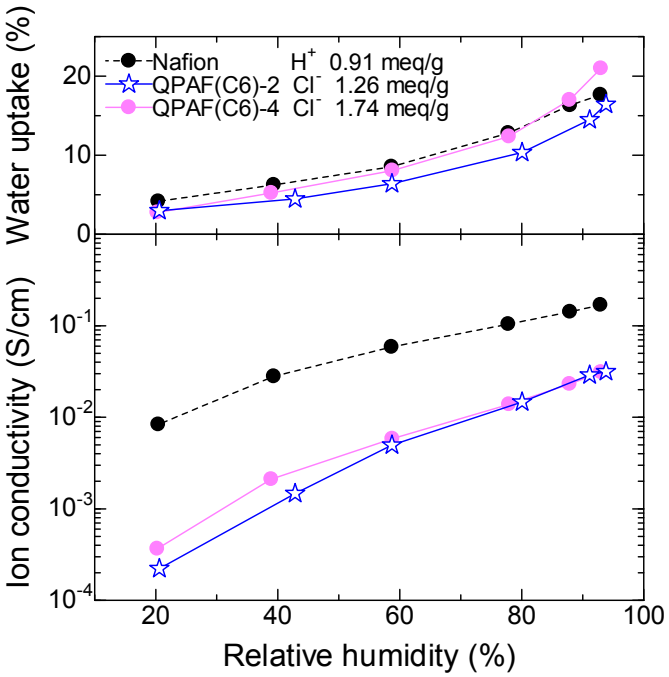

Fig. 6. Humidity dependence of water uptake and Cl^- conductivity of QPAF(C6)-2 and -4 membranes at 80 °C.

3.4 Alkaline Stability.

Alkaline stability of QPAF(C6)-2 (IEC = 1.26, Cl^- form) membrane was tested in 1 M KOH aqueous solution at 60 and 80 °C (**Fig. 7**). At 60 °C, the conductivity jumped from 8.4 mS/cm to 61.7 mS/cm in the first 24 h due to the ion exchange from Cl^- form to more conductive OH^- form. The conductivity decreased to 6.2 mS/cm at 400 h. At 80 °C, the decrease in the conductivity was faster and took place simultaneously with the ion exchange reaction. Therefore, the maximum conductivity was 20 mS/cm at 24 h and lower than that at 60 °C. The conductivity gradually decreased to 1.1 mS/cm in 500 h testing. For comparison, the conductivity of QPE-bl-9 (IEC = 1.3 meq/g) membrane with similar IEC value decreased from 6.7 mS/cm to 0.2 mS/cm after 500

h at 80 ºC,[17] implying similar alkaline stability for both membranes. The post-test QPAF(C6)-2 membrane retained its shape and bendability, however, lost solubility in organic solvents. In the IR spectrum of the post-test membrane, the peaks at 1738 cm^{-1} assignable to C-C stretching vibration in the aromatic rings and 891 cm^{-1} assignable to $C\text{-}N^{+}$ deformation vibration in the ammonium groups were smaller than those of the pristine membrane (**Fig. 8**). A new peak assignable to C-C deformation vibration was observed at 1562 cm^{-1}. The results suggest structural changes in the phenylene groups and the ammonium groups. The degradation of the ammonium groups accounts for the decrease in the conductivity during the alkaline stability test. While NMR and GPC analyses were not available due to its insolubility, the IR spectrum of the post-test membrane did not show evidences of degradation in the perfluoroalkylene groups.

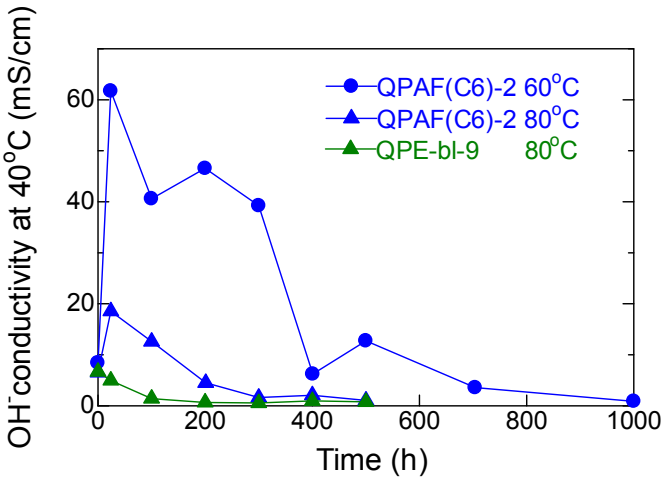

Fig. 7. Time course of hydroxide ion conductivity of QPAF(C6)-2 (IEC = 1.26 meq/g) and QPE-bl-9 (IEC = 1.3 meq/g) membranes in 1 M KOH aqueous solution at 60 and 80 °C.

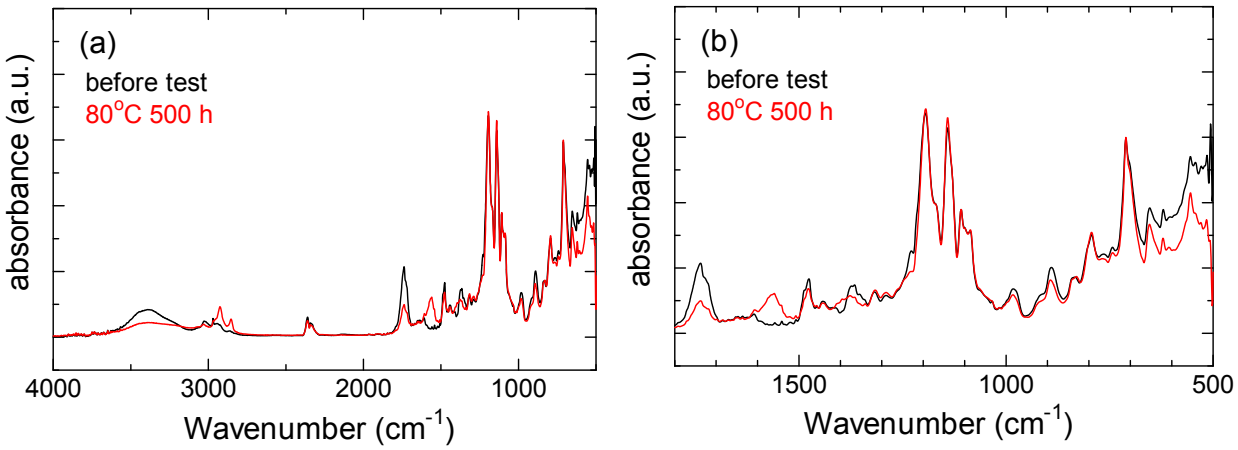

Fig. 8. IR spectra of QPAF(C6)-2 membrane (IEC = 1.26 meq/g) before and after the alkaline stability test in the range of (a) 500 - 4000 cm^{-1} and (b) 500 -1800 cm^{-1}.

3.5 Gas Permeability.

Hydrogen and oxygen gas permeabilities of QPAF and Nafion membranes were measured at 80 °C and plotted as a function of RH in **Fig. 9**. While both contained the perfluorinated aliphatic main groups in the main chain, QPAF membranes showed significantly lower hydrogen and oxygen permeability at wide range of humidity from 0 to 90% RH. The effect was more pronounced for oxygen than hydrogen; hydrogen and oxygen permeability of QPAF membranes was 13 - 26% and 5 - 12% that of Nafion at 90% RH, respectively. It is considered that the benzyl trimethylammonium moieties as hydrophilic component lower gas permeability and the hydrophobic perfluorinated component facilitate oxygen permeability. Similar gas permeability properties and dependencies have been observed for proton conducting ionomer membranes composed of aromatic polymers.[21] QPAF(C4)-1 with shorter perfluorinated chains exhibited lower gas permeability than that of QPAF(C6)-1, supporting this idea. The lowest hydrogen (1.1

× 10^{-9} cm^3 (STP) cm s^{-1} cm^{-2} $cmHg^{-1}$) and oxygen (5.9 × 10^{-11} cm^3 (STP) cm s^{-1} cm^{-2} $cmHg^{-1}$) permeability was achieved with QPAF(C4)-1 membrane at 0% RH. The gas permeability of QPAF membranes increased slightly with increasing humidity probably because absorbed water acted as a plasticizer to promote the gas permeation. QPAF membranes exhibited lower gas permeability than that of our reported aromatic multiblock co-polymers.[21,22] Smaller phase separated morphology of QPAF membranes would be responsible.

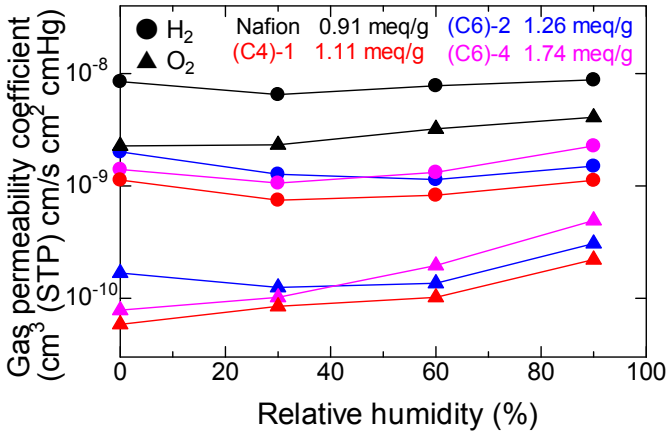

Fig. 9. Hydrogen and oxygen permeability of Nafion (in H^+ form) and QPAF (in Cl^- form) membranes at 80 °C as a function of RH.

3.6 Mechanical Properties.

Temperature dependence of the storage moduli (E'), loss moduli (E"), and tan δ of the QPAF membranes in Cl^- forms and Nafion membrane in H^+ form was measured at 60% RH (**Fig. 10**). Compared to QPE-bl-9, which exhibited nearly constant viscoelastic properties from room temperature to 95 °C,[17] QPAF and Nafion membranes showed decrease in the storage moduli as increasing the temperature. The storage modulus of QPAF(C6)-2 decreased from 1.01 × 10^9 Pa at 60 °C to 2.03 × 10^8 Pa at 95 °C, however, was still higher than that of Nafion at any temperature examined. QPAF(C6)-2 and Nafion membranes exhibited broad peaks in the loss moduli, which

might be associated with the glass transition. The results suggest that the perfluorinated aliphatic main chains could lower the thermomechanical properties. The larger water uptake of QPAF membranes than that of QPE-bl-9 membrane should also be responsible for the formers' lower mechanical properties. Such effect could be mitigated to some extent by shortening the aliphatic main chains; QPAF(C4)-1 showed less temperature dependence of the storage and loss moduli.

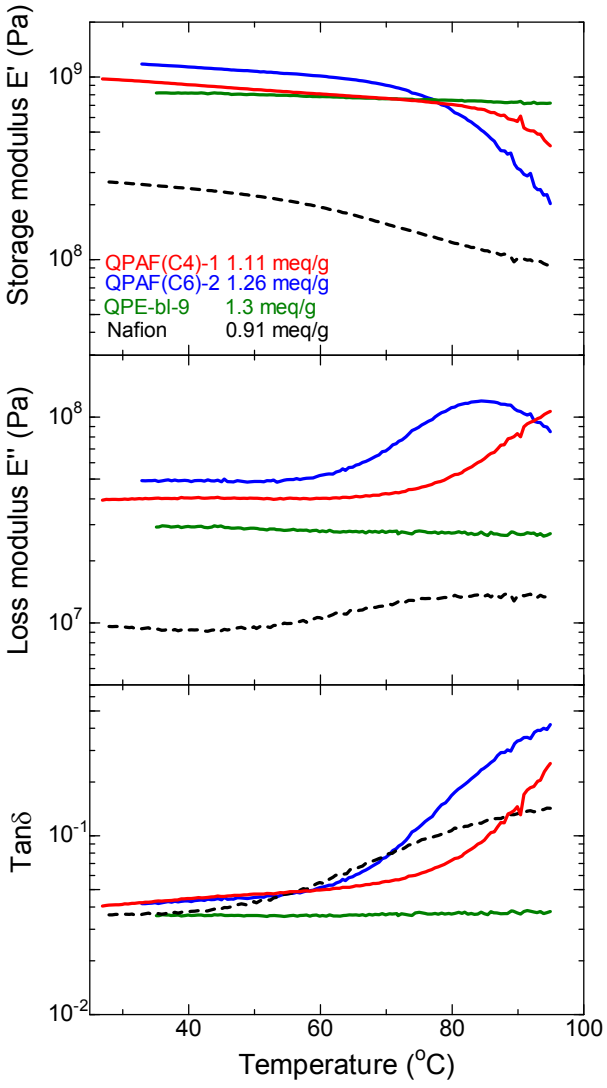

Fig. 10. DMA analyses of QPAF, QPE-bl-9 (both in Cl^- form), and Nafion (in H^+ form) membranes at 60% RH as a function of temperature.

The elongation tests were carried out for QPE-bl-9, QPAF and Nafion membranes at 80 °C, 60% RH (**Fig. 11**). QPAF(C6)-2 (IEC = 1.26 meq/g) exhibited considerably higher elongation at break (218%) and ca. 3.5 times higher yield stress (23.6 MPa) than those of QPE-bl-9 (5%, 6.7 MPa). Since differences in their molecular weight, IEC and water uptake values were rather small, such large differences in the elongation properties could be derived from the perfluoroalkylene groups. The QPAF(C4)-1 (IEC = 1.11 meq/g) with shorter perfluorolkylene groups in the main chain exhibited higher initial Young's modulus (0.23 GPa) and higher yield stress (27.3 MPa) than those of QPAF(C6)-2 but no plasticity after the yield point (elongation at break was as low as 5%), suggesting that the longer perfluoroalkylene groups contribute to the ductility of the membrane. QPAF(C6) membranes exhibited similar elongation behavior to that of Nafion with plasticity and large strain at break. The elongation at break of QPAF(C6) and Nafion membranes was in the reverse order of the IEC values; 404% for Nafion (IEC = 0.91 meq/g), 218% for (C6)-2 (IEC = 1.26 meq/g), and 149% for (C6)-4 (IEC = 1.74 meq/g).

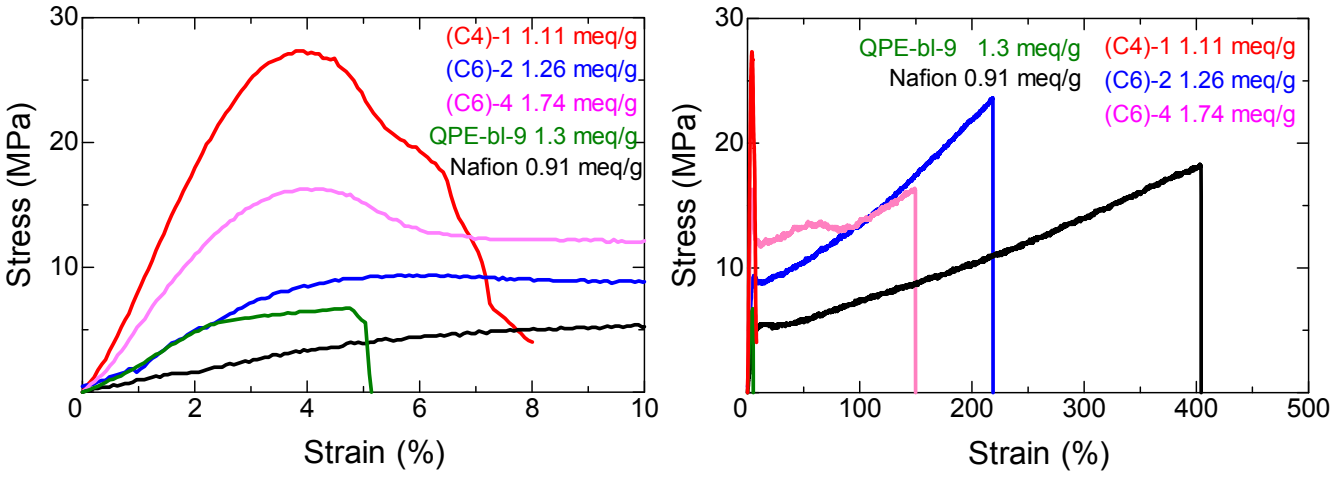

Fig. 11. Stress versus strain curves of QPAF (Cl^- form) and Nafion NRE212 (H^+ form) membranes at 80 °C and 60% RH.

3.7 Fuel Cell Performance.

The current density / voltage (I/V) and current density / power density (I/W) curves of the MEA is shown in **Fig. 12a**. The I/V data were collected after 4 h at 100 mA of conditioning and then the data was plotted every 5 minutes. The performance was stable during 3 cycles of the measurement and the data on the third cycle was adopted. The open circuit voltage (OCV) was 1.01 V, which was comparable to that (ca. 1.0 V) of an MEA with Nafion membrane with comparable thickness. The high OCV is indicative of low hydrogen permeation through the QPAF(C6)-2 membrane. The low gas permeability of QPAF membrane has been confirmed both in chloride form (see **Fig. 9**) in ex-situ experiments and in hydroxide ion form in an operating fuel cell. The ohmic resistance was nearly constant (ca. 0.3 Ω cm^2) at any current density (**Fig. 12b**). It was 3.3 times higher than that (0.09 Ω cm^2) estimated from the hydroxide ion conductivity of the membrane (58.5 mS/cm in water at 40 °C) possibly because of lower conductivity of the membrane in fully humidified gases than in water. It may contain the contact resistance between the membrane and the catalyst layers. The fuel cell exhibited the maximum power density of 139 mW/cm^2 at a current density of 420 mA/cm^2. The maximum power density obtained herein was not state-of-the-art compared to the literature works.[6,7] Nevertheless, the result was highly promising taking into account the operating conditions with low Pt loading amount (0.2 mg/cm^2) and no back pressure for hydrogen and oxygen supply. Fuel cell was also operated with QPAF(C6)-4 membrane with higher IEC (1.74 meq/g) under the same conditions. The maximum power density slightly improved by elevating the operating temperature from 40 °C (110 mW/cm^2) to 60 °C (138 mW/cm^2) (**Fig. S7** in the ESI †).

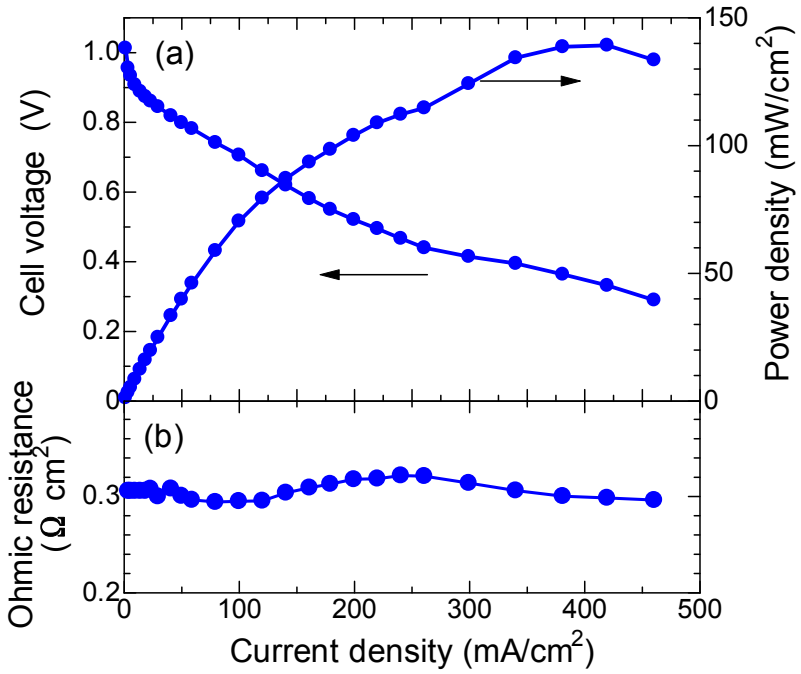

Fig. 12. (a) Fuel cell performance and (b) ohmic resistance of MEA using QPAF(C6)-2 as membrane and electrode binder at 40 °C.

4. Conclusions

We have designed and synthesized ammonium functionalized copolymers (QPAFs) composed of perfluoroalkylene and phenylene main chains without heteroatom linkages. The polymerization, chloromethylation, and quaternization reactions were quantitative to provide high molecular weight copolymers with controllable IEC value. QPAFs thus obtained were soluble in a variety of polar organic solvents such as methanol, DMF, and DMSO, and provided bendable membranes by solution casting. Because of the significant hydrophilic/hydrophobic differences in the main chain between the perfluoalkyl and the quaternized phenylene groups, the random copolymers exhibited distinct phase-separated morphology as suggested by TEM images. The

QPAF membranes exhibited a volcano type dependence of the hydroxide ion conductivity on the IEC, and the balanced conductivity and water uptake properties were obtained for the QPAF membrane with IEC = 1.26 meq/g. Because of the lack of heteroatom linkages in the main chains, QPAF membranes showed reasonable stability in water and alkaline solution at 80 °C. However, the benzyl trimethylammonium groups were decomposed in hot 1 M KOH resulting in a decrease in the conductivity within several hundred hours. QPAF and Nafion membranes, both containing perfluorinated alkylene groups in the main chain, exhibited similar mechanical properties, while QPAF membrane showed much lower gas permeability presumably because of the rigid phenylene units attached with the ammonium groups. A fuel cell using the QPAF as membrane and electrode binder was successfully operated with humidified hydrogen and oxygen (no back pressure). The maximum power density obtained was 139 mW/cm^2 at the current density of 420 mA/cm^2, proving that the QPAF functioned well in an operating fuel cell.

Acknowledgements

This work was partly supported by the Ministry of Education, Culture, Sports, Science and Technology (MEXT) Japan through a Grant-in-Aid for Scientific Research (26289254).

Notes and references

[a]Interdisciplinary Graduate School of Medicine and Engineering, [b]Fuel Cell Nanomaterials Center, and [c]Clean Energy Research Center, University of Yamanashi, 4 Takeda, Kofu, Yamanashi 400-8510, Japan

[d]Japan Science and Technology Agency, CREST, 4-1-8 Honcho, Kawaguchi, Saitama 332-0012, Japan

† Electronic supplementary information (ESI) available: Detailed characterization of monomers, PAFs, CMPAFs, and structure of QPE-bl-9. See DOI: 10.1039/x0xx00000x

1 L. Carrette, K. A. Friedrich and U. Stimming, *Fuel Cells*, 2001, **1**, 5-39.

2 K. D. Kreuer, *Chem. Mater.*, 2014, **26**, 361-380.

3 A. Kraytsberg and Y. Ein-Eli, *Energy Fuels*, 2014, **28**, 7303-7330.

4 C. G. Arges, V. Ramani and P. N. Pintauro, *ECS Interface*, 2010, **19**, 31-35.

5 G. Merle, M. Wessling and K. Nijmeijer, *J. Membr. Sci.*, 2011, **377**, 1-35.

6 J. R. Varcoe, P. Atanassov, D.R. Dekel, A. M. Herring, M. A. Hickner, P. A. Kohl, A. R. Kucernak, W. E. Mustain, K. Nijmeijer, K. Scott, T. Xu and L. Zhuang, *Energy Environ. Sci.*, 2014, **7**, 3135-3191.

7 S. Lu, J. Pan, A. Huang, L. Zhuang and J. Lu, *Proc. Natl. Acad. Sci. USA*, 2008, **105**, 20611-20614.

8 J. Miyake, M. Watanabe and K. Miyatake, *Polym. J.*, 2014, **46**, 656-663.

9 N. Li, Y. Leng, M. A. Hickner and C.-Y. Wang, *J. Am. Chem. Soc.*, 2013, **135**, 10124-10133.

10 X. Ren, S.C. Price, A. C. Jackson, N. Pomerantz and F. L. Beyer, *ACS Appl. Mater. Interfaces*, 2014, **6**, 13330-13333.

11 W. H. Lee, A.D. Mohanty and C. Bae, *ACS Macro Lett.*, 2015, **4**, 453-457.

12 M. Tanaka, M. Koike, K. Miyatake and M. Watanabe, *Macromolecules*, 2010, **43**, 2657-2659.

13 M. Tanaka, K. Fukasawa, E. Nishino, S. Yamaguchi, K. Yamada, H. Tanaka, B. Bae, K. Miyatake and M. Watanabe, *J. Am. Chem. Soc.*, 2011, **133**, 10646-10654.

14 C. Fujimoto, D. S. Kim, M. Hibbs, D. Wrobleski and Y. S. Kim, *J. Membr. Sci.*, 2012, **423**, 438-449.

15 Y. K. Choe, C. Fujimoto, K. S. Lee, L. T. Dalton, K. Ayers, N. J. Henson and Y. S. Kim, *Chem. Mater.*, 2014, **26**, 5675-5682.

16 C. G. Arges and V. Ramani, *Proc. Natl. Acad. Sci. USA*, 2013, **110**, 2490-2495.

17 N. Yokota, M. Shimada, H. Ono, R. Akiyama, E. Nishino, K. Asazawa, J. Miyake, M. Watanabe and K. Miyatake, *Macromolecules*, 2014, **47**, 8238-8246.

18 P. Bhattacharyya, D. Gudmunsen, E. G. Hope, R. D. W. Kemmitt, D. R. Paige and A. M. Stuart, *J. Chem. Soc., Perkin Trans., 1* 1997, **24**, 3609-3612.

19 A. Bastero, G. Francio, W. Leitner and S. Mecking, *Chem. Eur. J.*, 2006, **12**, 6110-6116.

20 D. W. Seo, M. A. Hossain, D. H. Lee, Y. D. Lim, S. H. Lee, H. C. Lee, T. W. Hong and W. G. Kim, *Electrochim. Acta*, 2012, **86**, 360-365.

21 B. Bae, T. Hoshi, K. Miyatake and M. Watanabe, *Macromolecules*, 2011, **44**, 3884-3892.

22 N. Yokota, H. Ono, J. Miyake, E. Nishino, K. Asazawa, M. Watanabe and K. Miyatake, *ACS Appl. Mater. Interfaces*, 2014, **6**, 17044-17052.

Graphical Abstract

Anion exchange membranes composed of perfluoroalkylene chains and ammonium-functionalized oligophenylenes

Hideaki Ono,[ad] Junpei Miyake,[cd] Shigehumi Shimada,[a]
Makoto Uchida,[bd] and Kenji Miyatake*[bcd]